The design of a shaking table campaign on the out-of-plane response of masonry structures

Dario Vecchio[1*], *Carla* Colombo[1], Georgios *Vlachakis*[1], *Nuno* Mendes[1] and *Paulo B.* Lourenço[1]

[1]University of Minho, ISISE, ARISE, Department of Civil Engineering, Guimarães, Portugal

Abstract. Despite the widespread presence in earthquake-prone areas, unreinforced masonry heritage buildings are significantly vulnerable to seismic events. Among the possible failures, the out-of-plane mechanism poses the greatest potential for collapse and involves inherent complexities. In particular, one-way and two-way bending are significantly recurrent yet not fully understood mechanisms, thus requiring further in-depth investigations. Such mechanisms can be idealized as single- or multi-rigid bodies experiencing rotational motions around two pivot points at the base. Albeit engineering applications are still limiting their approach to the use of static tools, the current research studies seek to forecast the dynamic behaviour of structures during the complete time history of any seismic actions. Nevertheless, it is apparent the necessity of experimental evidence to support the development of more advanced models capable of closely predicting the out-of-plane response. This paper presents the design of an extensive shaking table experimental campaign conducted at the Structural Laboratory of the University of Minho (Portugal), within the scope of the STAND4HERITAGE (New Standards for Seismic Assessment of Built Cultural Heritage) project. The campaign envisages the study of the dynamics of dry-joint masonry structures subjected to out-of-plane actions. The goal is to enlarge the experimental database currently available in the literature and to provide data for the validation of analytical and numerical models.

1 Introduction

Post-earthquake observations of the damage experienced by traditional unreinforced masonry structures (URM) have demonstrated that the most recurring failure mechanism under dynamic actions is the out-of-plane (OOP) overturning of façade walls [1]. Such failure can be resembled by a rigid body motion, with a portion of the façade detaching from the rest of the structure [2], resulting either in local or global failure mechanisms. Despite the variety of parameters involved, such as the material properties, aspect ratios, type of interlocking, presence of openings and many others, these mechanisms are crucially influenced by their

* Corresponding author: dariovecchio4@yahoo.it

These proceedings are published with the support of EuLA.

boundary conditions. Accurately predicting the actual mechanism in real structures is a challenging task, and many assumptions are often adopted. However, recent observations of post-earthquake reconnaissance ([3], [4]) have revealed the major occurrence of two types of OOP mechanisms, namely one-way and two-way bending. The former can refer to the motion experienced by a façade without any side or diaphragm restraints, which rotate around the bottom interface (**Fig. 1a**). Alternatively, if diaphragm restrain is present at the top, the façade might experience vertical bending, leading to the development of horizontal cracks at an intermediate height (i.e. vertical spanning strip walls, **Fig. 1b**). Finally, the two-way bending mechanism occurs when a combined action between vertical and horizontal bending arises, and it is observed for walls with the horizontal and the vertical edge restrained (**Fig. 1c**).

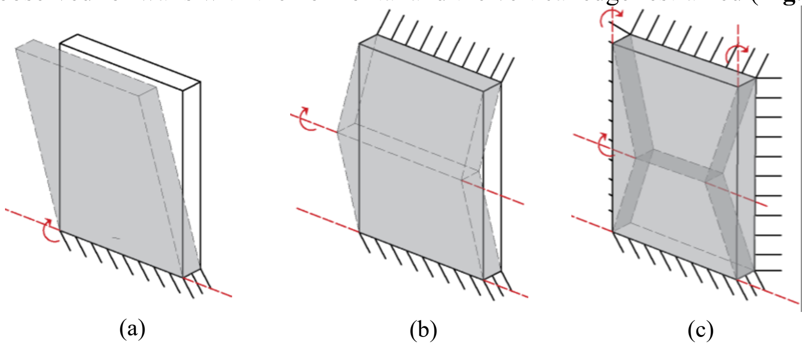

Fig. 1. Out-of-plane mechanisms: (a) one-way response of a cantilever wall, (b) one-way response of a vertical spanning strip wall, (c) two-way bending of wall restrained at the top and sides.

The mechanisms have been examined in several analytical and numerical investigations. Up to date, force- and displacement-based static approaches are still the main methodologies that most practitioners use to estimate the cracking peak force and the ultimate displacement. However, it is widely accepted that such methods neglect the dynamic phenomena of the OOP mechanisms and thus do not provide reliable accuracy and tend to overestimate strengthening or repair solutions [5]. On the contrary, the classical rocking dynamic theory states the dynamic problem of the planar rigid body rocking over two pivot points (as shown in **Fig. 2**). To this end, it solves the equation of motion under a time history loading and provides a better insight of the complex non-linear response. Nonetheless, this approach is limited to two-dimensional representations while three-dimensional effects are neglected. Therefore, advanced numerical finite element of discrete element models provides the most reliable approach to analyse such mechanisms. Such models usually adopt a block-based representation of masonry with contact interfaces dictating their interaction. Nevertheless, these models often become impracticable due to the complexity of the constitutive laws required, together with their significantly high computational cost [5].

Many authors are investigating the field of rocking dynamics applied to URM structures, and the creation of new analytical formulations is continuously under discussion. However, due to the high non-linearity and sensitivity of the rocking phenomenon to many parameters, the accuracy of these models is still limited. Ensuring the reliability of these models requires the calibration and validation against experimental outcomes. Despite this necessity, laboratory data, particularly from shaking table tests—recognized as the most advanced tool for simulating seismic actions—remains scarce in the literature. In this paper, an extensive shaking table campaign within the framework of the S4H project is presented. It aims to investigate the one-way and two-way bending mechanisms by testing half-scale specimens made of granite blocks. In the following sections, the campaign is presented, including the description of the shaking table facility, the testing methods, the description of the test setup and the expected outcomes. Finally, conclusions are drawn to summarize the objectives and the novelties of the experimental campaign.

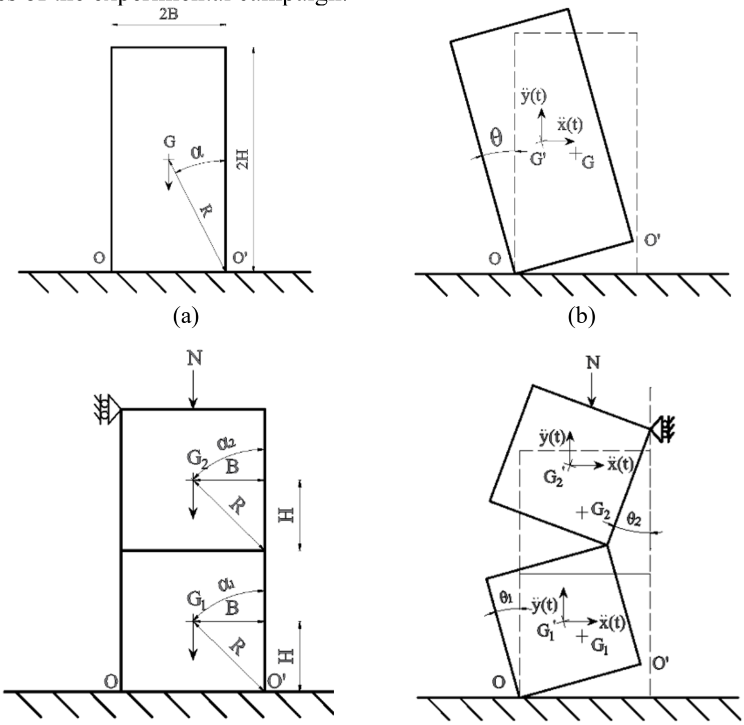

Fig. 2. Single (a-b) and multi-blocks (c-d) rocking systems: (a, c) undeformed configurations, and (b, d) deformed configurations.

2 Shaking table facility

The experimental campaign is conducted at the structural engineering laboratory of the University of Minho in Guimarães, Portugal. The shaking table employed in the campaign is unidirectional and has a dimension of 2.9 m x 2.9 m. It is provided with a controlling station of two chassis, with the first in charge of operating the system and the hydrodynamic actuator, while the second as a possible expansion. The first chassis is provided with 16 analogue inputs to allow the connections of any wire or powered transducers. The shaking table surface is equipped with a grid of M27 holes, facilitating direct bolted connections between the table and the specimens. In addition, the table is provided with an accelerometer PCB 393A03, capable of measuring in the range of ±5g. The hydrodynamic actuator can operate under a maximum pressure of 280 bars and with a stall load nominal capacity of 312 kN. The allowed range of frequencies spans from 0 to 50 Hz, which covers the frequency range of interest for masonry structures. **Table 1** summarises the main features of the shaking table, while **Fig. 3** shows a view of the platform and the actuator.

Table 1. Shaking table characteristics.

Size [mm^2]	Frequency [Hz]	PTD^a [mm]	PTV^b [mm/s]	PTA^c [g]	$M_{ST}{}^d$ [kg]	$M_{MAX}{}^e$ [kg]
(2900 x 2900)	0-50	±125	850	5	3000	3000

PTD^a = Peak Table Displacement, PTV^b = Peak Table Velocity, PTA^c = Peak Table Acceleration, $M_{ST}{}^d$ = Shaking Table Mass, $M_{MAX}{}^e$ = Maximum payload.

Fig. 3. View of the shaking table facility.

In addition, a six-cameras Digital Image Correlation (DIC) acquisition system is installed in the perimetrical area of the shaking table. The DIC is an optical method which allows the recording of a full field contour of displacement of an object over time, without interfering with the system dynamics. The DIC cameras record relative translations of an image subset between two consecutive pictures, allowing the creation of a displaced configuration at each time step. To do so, the region of interest must be covered with a speckle pattern, either glued or spray painted. The pattern should have a random distribution of the grid points, uniform size, with good grey-scale contrast, and no aliasing between pixels.

3 One-way bending mechanism

3.1 The Vertical Spanning Strip Wall

The Vertical Spanning Strip Wall (VSSW) mechanism appears when a façade is provided with sufficient translational restrain at the diaphragm's levels (roof or slab), and either it is located near an opening, or it lacks proper connection with the return walls. In such case, if the seismic action is sufficient to trigger the motion, three hinges will occur: one at the base, one at the top and one at an intermediate height of the wall, forming the VSSW mechanism (**Fig. 2c, d**). The behaviour of this mechanism can be idealised as a double rigid body motion pivoting around the top and bottom edge connections, and around the hinge that forms along the height of the panel. Moreover, by considering displacement compatibility among the blocks and the boundary conditions, this mechanism can be analysed using solely one generalised degree of freedom, commonly chosen to be the rotation of the base block. Assuming that friction is sufficient to prevent sliding between the blocks [6], if the ground acceleration $\ddot{u}_g$ equals or exceeds the restoring moment given by the gravitational forces, the system will start oscillating around the pivot points. During these oscillations, the blocks will experience impacts with the ground and with each other, and consequently rotate around the opposite pivot. These impacts occur in very short time intervals, during which impulsive forces are generated, causing energy losses. As a result, the motion gradually decreases in amplitude, as the system dissipates its energy through these impacts. Sorrentino et al. [7] derived the EOM of this mechanism using Lagrangian dynamics. More specifically, by considering as independent DOF the rotation of the bottom body, and expressing the rotation of the upper body as a function of the former, the equation of motion can be written as:

$$R_1 C_A \ddot{\theta}_1 + \mathrm{sgn}(\theta_1) R_1 C_S \dot{\theta}_1^2 = -\ddot{x}(t) C_H + \mathrm{sgn}(\theta_1)\left[\ddot{y}(t) - g\right] C_V - \mathrm{sgn}(\theta_1) N C_N \quad (1)$$

where C_A, C_S, C_H, C_V and C_N are system coefficient functions of the rotation of the bottom body θ_1. For a more detailed mathematical description of these parameters, the reader can refer to [7]. In addition, the energy losses occurring during the impacts can be estimated using the conservation of angular momentum. Hence, the same authors equated the angular momentum before and after the impact in order to compute the ratio between the angular velocities after and before the impact:

$$\frac{\dot{\theta}_1^+}{\dot{\theta}_1^-} = \frac{m_1 R_1^2 + I_{G,1} - I_{G,2}\dfrac{\tan\alpha_2}{\tan\alpha_1} - 2 m_1 R_1^2 \sin^2\alpha_1 + m_2 R_1^2\left[2 + \dfrac{\sin\alpha_1\cos\alpha_1}{\tan\alpha_2} - \sin^2\alpha_1\left(4 + \dfrac{\tan\alpha_2}{\tan\alpha_1}\right)\right]}{m_1 R_1^2 + I_{G,1} - I_{G,2}\dfrac{\tan\alpha_2}{\tan\alpha_1} + m_2 R_1^2\left[2 + \sin\alpha_1\cos\alpha_1\left(\dfrac{1}{\tan\alpha_2} + \tan\alpha_2\right)\right]} \quad (2)$$

In literature, this is known as the Coefficient of Restitution (CoR), usually denoted as *e* or *r*. This has been the core of investigations of many authors, who attempted at calibrating this quantity versus experimental data. However, due to the extremely small duration of each impact, the non-perfect parallelepiped assumptions of the blocks, the geometric uncertainties at the contact surfaces and others, this task remains an open and especially challenging topic.

3.1.1 Test setup

The present subsection intends to describe the experimental setup designed to achieve the occurrence of the one-way bending mechanism under dynamic actions (**Fig. 2c, d**). To consider the variability of masonry façades, two wall aspect ratios H/B (height/width), are herein considered, i.e. 15 and 13.75, with H being the total height and B the width of the specimen, respectively A single leaf wall was built with granite blocks, each of 625 mm x 125 mm x 100 mm nominal dimensions, while a larger block of nominal dimensions 1665 mm x 165 mm x 165 mm constitutes the base boundary condition. The base block was drilled along the height to ensure the fixity to the shaking table with two threaded bolts (**Fig. 4**).

Fig. 4. The VSSW setup: close view of the base boundary condition. The red-dashed circle highlights the connection between the base block and the shaking table.

Concerning the top boundary conditions, a 260 HEA steel beam is used to transmit the shaking table action on the top boundary condition of the specimen and at the same time apply a distributed overburden load. The top beam is connected to the external retaining frame by means of struts and sliders (**Fig. 5a**). The retaining frame consists of four IPE columns stiffened by same-size diagonals, which are welded to base steel plates, in turn bolted to the shaking table. The top beam is connected to a top block (625 mm x125 mm x 125 mm) using chemical anchors bolted to the bottom flange of the beam. Additionally, stiffened L-profiles are bolted to the beam and placed on the block sides to provide a mechanical rotational constraint (**Fig. 5b**). Note that the system created by the top beam and the top block is designed only to displace vertically but not rotate during the tests to allow the hinge opening at the top of the specimen's height. In order to ensure no relative rotation, the two L-profiles are connected to rollers designed to be in perfect contact with the interior side of the IPE column (**Fig. 5b**), thus allowing the top beam-block system only to uplift. The details of this connection are shown in **Fig. 5 a, b**.

(a)

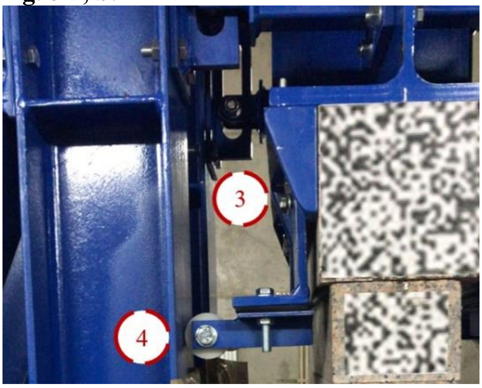

(b)

Fig. 5. The VSSW top boundary conditions: (a) top beam-column zoom view and (b) L-profiles and roller system. In Fig. 5a, detail (1) shows the slider connection, while detail (2) the chemical anchors connecting the bottom flange of the top beam with the masonry top block. In Fig. 5b, detail (3) shows the stiffened L-profile and (4) the roller in touch with the interior side of the IPE column.

To simulate a representative overburden level for masonry structures, the setup included a system of four extension springs, two tubular profiles, four load cells, and four threaded bars. Note that the level of pre-compression σ_p was designed to vary from 0 MPa to 0.05 MPa. The springs have been designed with a stiffness of 2 kN/m, thus ensuring a practically constant compression stress on top of the wall during the test. Furthermore, they are connected in pairs through the hollow profiles, which are in turn placed on the top flange of the 260 HEA beam. The tubular profile was designed with two M16 holes at each end to allow for the insertion of a threaded bar (**Fig. 6a**) connecting the springs and load cells (**Fig. 6b**).

Finally, each spring was anchored to its respective steel plate with a hook welded at the base. For a complete picture, **Fig. 7** shows an overview of the VSSW setup, including a schematic 3d view of the blocks' orientations, and nominal dimensions.

The campaign envisions the testing of the wall under free and forced excitations. More specifically, the free motion of the wall is triggered by a Ricker wavelet and permits the characterisation of the energy losses occurring during impact. Additionally, the forced rocking motion of the wall is studied, accounting for variations in terms of wall aspect ratio H/B, overburden load and ground motion input. An overview of the VSSW campaign can be found in **Table 2**.

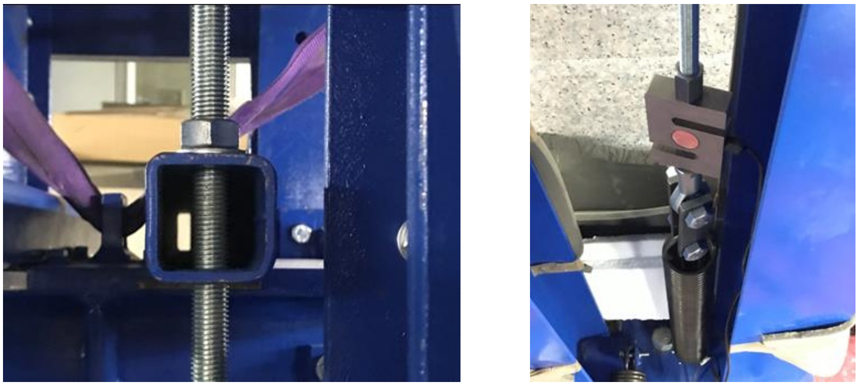

(a) (b)

Fig. 6. The VSSW pre-compression system: (a) detail of the vertical threaded bar and the tubular profile, and (b) the extension spring-load cell connection.

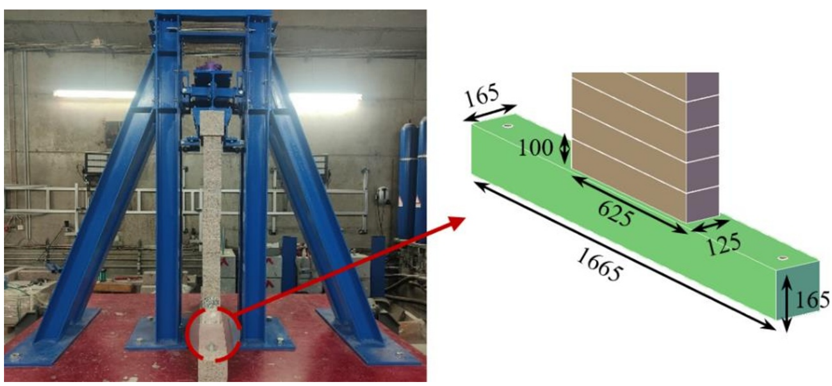

Fig. 7. The VSSW setup: general view and orientation of the blocks. Dimensions are in mm.

Table 2. Main features of the shaking table testing of the VSSW.

	Free rocking		Forced rocking	
H/B [-]	13.75	15	13.75	15
σ_p [MPa]	0/0.025/0.05		0/0.025/0.05	
Signal type	Ricker wavelet		Ground motions	
No. of tests	3 (each)		IDA[a]	

IDA[a] = Incremental Dynamic Analysis.

3.1.2 Choice of the input ground motion

This sub-section briefly describes the choice of the input signals to induce the desired mechanism. The main objectives of this test are the observation of the rocking motion and the quantification of the energy dissipation mechanism due to impacts. To this end, two types of excitations are employed, respectively (**Table 2**): i) Ricker wavelets in order to trigger the free-rocking response, and ii) recorded ground motions to study the forced-rocking response. More specifically, the free rocking motion is initiated using a Ricker wavelet pulse, artificially created for several angular frequencies f_M and amplitudes $f(t)$, following the formulation:

$$f(t) = (1 - 2\pi^2 f_M^2 t^2) e^{-\pi^2 f_M^2 t^2} \quad (3)$$

Regarding the forced-rocking tests, the choice of a suitable accelerogram had to comply with the limitations posed by the shaking table in terms of PTD, PTA and PTV (refer to **Table 1**). Consequently, the response of the VSSW against alternative candidate ground motions was simulated numerically using **Eq. 1**. Incremental Dynamic Analyses (IDA) were carried out for several ground motions and the signal that provided a smooth incremental behaviour was selected. Note that the response of such systems is extremely sensitive and thus it commonly produces highly weaving IDA curves with pronounced variability [8]. **Table 3** summarises some key features of the four ground motions selected to ensure a smooth incremental behaviour.

Table 3. Some key features of the selected ground motions for the shaking table tests on the VSSW.

Event ID	Event date	Mw^a	D^b [km]	PGA^c [g]
IT-2012-0032	2012-05-29	5.5	6.9	0.19
IT-1990-0003	1990-12-13	5.6	46.7	0.21
GR-1999-0001	1999-09-07	5.9	21.1	0.23
GR-1993-0027	1993-07-14	5.6	4.9	0.18

Mw^a = moment magnitude, D^b = epicentral distance, PGA^c = Peak Ground Acceleration.

3.2 Facade overturning and return wall shear failure

Differently than above, URM façades might be provided with sufficient restrain only at their base, while the top portion might be free to detach from the rest of the structure. Depending on the presence and on the connectivity offered by the return walls, a variety of mechanisms might arise. Specifically in the case of a weak connection with the return wall, a vertical crack might appear, thus detaching the façade from the side walls. This motion can be represented as a one-sided rocking system, as shown in **Fig. 8**. Note that the mechanism shown in **Fig. 2a, b** identifies a two-sided rocking system.

The equation of motion for this mechanism is identical to that of a two-sided rocking wall:

$$\ddot{\theta} = -p^2 \left[\operatorname{sgn}(\theta)\sin(\alpha - |\theta|) + \frac{\ddot{x}(t)}{g}\cos(\alpha - |\theta|) \right] \quad (4)$$

Nevertheless, in the case of one-sided, during impacts the rocking wall collides also with the return wall, thus provoking a significant energy loss [9]. It is straightforward to see how the above formulation simply refers to a cantilever free to rock over its base. Indeed, such formulation was used to predict the response of the cantilever mode in previous experiments. However, this mechanism may be highly influenced by the presence of return walls. Indeed, if the interlocking at the connection with the return wall provide some moment connection and without proper return wall-to-diaphragm connection, a diagonal crack may propagate diagonally from the lower vertex of the corner to the top edge of the return walls. The cracking contribution is clearly lacking in the above formulation, likely resulting in wrong estimation of the time history response of the system. As a result, the design test setup and the choice of the proper accelerogram cannot completely rely on the analytical formulations given in **Eq. 4**.

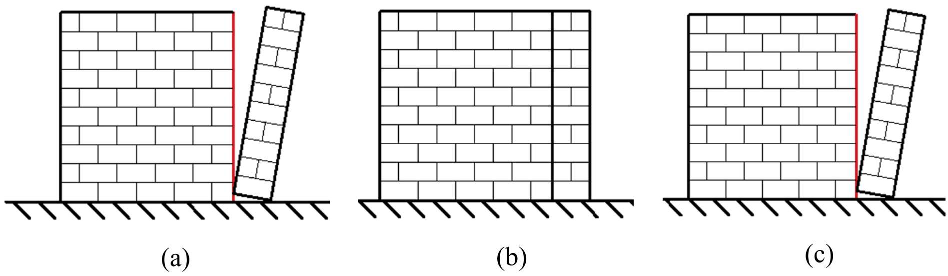

Fig. 8. Cantilever façade experiencing one-sided rocking motion, with impacts occurring between the façade and the return wall. In detail, (a) happens first, next (b), and finally (c).

3.2.1 Design of test setup

To evaluate experimentally the one-way bending of a URM façade, initial considerations were based on the discussion given above. More specifically, such mechanism initiates with a simple rocking of the façade up to the complete overturning and may include the return walls. Hence the specimen must be constructed in a U-shape fashion, with a slender façade and two orthogonal walls. Considering the limitation in size and capabilities of the shaking table, a half-scale specimen was designed with a slender façade and two strong return walls. The final geometric features of the specimen are summarized in **Table 4**.

Table 4. Geometrical properties of the U-shape specimen for the shaking table tests on the cantilever façade response (cantilever type).

OOP Façade			Return walls		
H [m]	L [m]	B [m]	H [m]	L [m]	B [m]
1.5	1.65	0.15	1.5	1.65	0.15

Given the comparable mass of the specimens and the shaking table, the connection between the specimen and the shaking table was designed to be as lightweight as possible. Steel plates were designed to be adequately connected to the table with 2M27 bolted connections. Furthermore, translational and rotational constraints were imposed on the first course of the specimen using two M16 threaded bolts hidden inside each block and firmly connected to the plate below. Careful attention was drawn to keeping the interface between first and second masonry course intact. Moreover, in order to avoid any sliding, and to improve the behaviour of the return walls, two systems of pre-compressed springs were designed to apply a vertical overburden load on the final edge of the return walls. The level of compression is accounted as a realistic overload that usually stands at the last floor of a URM structure, where such mechanism is likely to happen [1]. A picture of the final design is illustrated in **Fig. 9**, where the steel plates and the system of pre-compressed springs with hollow profiles are shown in blue, while the expected mechanism including shear failure in the return walls is shown in dark grey.

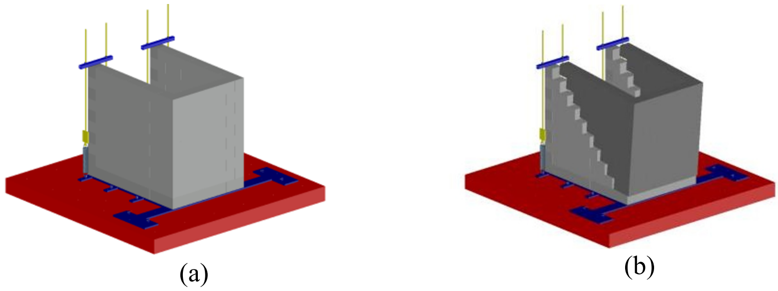

Fig. 9. The U-shape specimen for the shaking table test on the façade's cantilever response and shear failure of the return walls.

4 Conclusions

Research has shown that out-of-plane failure mechanisms are predominant and pose the major threat to the safety of historic and modern unreinforced masonry structures. Past *in-situ* observations have revealed the recurrent occurrence of two types of mechanism, namely one-way and two-way bending. These mechanisms pose a complex dynamic behaviour, which is particularly challenging to predict. More specifically, analytical rocking dynamics provide a reliable modelling scheme solely for simple mechanisms and with a series of assumptions, while advanced numerical approaches require many unknown input parameters and at the same time have a high computational cost. Importantly, the accuracy, reliability and calibration of these models should be based on experimental campaigns. To this end, this paper presents the design of an extensive experimental campaign about out-of-plane masonry structures. The campaign will be conducted with the shaking table that was recently installed at the University of Minho in order to meet the expected goals of the STAND4HERITAGE project. More specifically, two different types of tests will be conducted aiming at reproducing out-of-plane mechanisms, namely the vertical spanning strip wall and the one-way bending of a façade with side walls. For each mechanism, forced vibration tests, with the use of selected input ground motions, are to be conducted. Such tests will allow the direct observation of the rocking motion and the energy dissipation mechanisms. Finally, it is envisaged that the outcomes of the tests will be used to validating and calibrating analytical and numerical models for predicting the complex dynamic response of these mechanisms.

References

1. D. D'Ayala, R. Spence, C. Oliveira, A. Pomonis, Earthquake Loss Estimation for Europe's Historic Town Centres. Earthq. Spectra. **13**, (1997). https://doi.org/10.1193/1.1585980
2. G. De Felice, R. Giannini, Out-of-plane seismic resistance of masonry walls. J. Earthq. Eng. **5**, (2001). https://doi.org/10.1080/13632460109350394
3. D. Dizhur, J. Ingham, L. Moon, M. C. Griffith, A. Schultz, I. Senaldi, G. Magenes, J. Dickie, S. Lissel, J. Centeno, C. Ventura, J. Leite, P. B. Lourenço, Performance of masonry buildings and churches in the 22 February 2011 Christchurch eartquake. NZSEE. **44**, (2011). https://doi.org/10.5459/bnzsee.44.4.279-296
4. L. Moon, D. Dizhur, I. Senaldi, H. Derakhshan, M. Griffith, G. Magenes, J. Ingham, The Demise of the URM Building Stock in Christchurch during the 2010-2011 Canterbury Earthquake Sequence. Earthq. Spectra. **30**, (2014). https://doi.org/10.1193/022113EQS044M

5. S. Lagormarsino, Seismic assessment of rocking masonry structures. Bull. Earth. Eng. **13**, (2015) https://doi.org/10.1007/s10518-014-9609-x.
6. M. Aslam, W.G. Godden, D.T. Scalise, Earthquake Rocking Response of Rigid Bodies. J. Struct. Eng. (ASCE). **106**, (1978) https://doi.org/10.1061/JSDEAG.0005363
7. L. Sorrentino, R. Masiani, M. C. Griffith, The vertical spanning strip wall as a coupled rocking rigid body assembly. Struct. Eng. Mech. **29**, (2008). doi:10.12989/sem.2008.29.4.433.
8. C. G. Lachanas, D. Vamvatsikos, Rocking incremental dynamic analysis. Earth. Eng. Struct. Dyn. **51**, (2022). https://doi.org/10.1002/eqe.3586
9. L. Sorrentino, O. Al Shawa, L. D. Decanini, The relevance of energy damping in unreinforced masonry rocking mechanisms. Experimental and analytical investigations. Bull Earth. Eng. **9**, 2011. https://doi.org/10.1007/s10518-011-9291-1
10. L. Sorrentino, R. Masiani, L.D. Decanini, Overturning of rocking rigid bodies under transient ground motions. Struct. Eng. Mech. **22**, (2006). https://doi:10.12989/sem.2006.22.3.293.